EXPERIMENTS ON BEACH PROFILE CHANGE WITH A LARGE WAVE FLUME

By

Ryoichi Kajima*, Takao Shimizu**

Kohki Maruyama** and Shozo Saito***

ABSTRACT

Two-dimensional beach profile changes were investigated with a newly constructed prototype-scale wave flume. The flume is 205 m long, 3.4 m wide and 6 m deep. Sand of two grain sizes was used in the experiments. Analysis of the results was made through use of the parameter C, introduced by Sunamura and Horikawa (1974) to classify beaches as either erosional and accretionary. Beach profile changes obtained in the flume were similar to those in the prototype (field). Net sand transport rate distributions were classified into five types, two of which do not seem to have been observed in laboratory (small-scale) experiments. A simple model describing the five types was developed for evaluating two-dimensional beach profile changes.

INTRODUCTION

Construction of harbor and cooling water facilities of power stations can produce significant changes along the coast. Consequently, the development of coastal change prediction methods is very important to maintain the functions of these coastal structures and to preserve the coastal environment. In particular, studies on two-dimensional beach profile changes resulting from cross-shore sand transport occupy a very important position. However, most of the numerous investigations and results concerning two-dimensional beach changes have been based mainly on rather small-scale experiments. The consequences of unavoidable scale effects associated with these experiments are not easy to determine.

---

* Manager of Coastal Hydraulics Section, Civil Engineering Laboratory, Central Research Institute of Electric Power Industry (CRIEPI), 1646 Abiko, Abiko City, Chiba, 270-11 Japan.
** Research Engineer, CRIEPI.
*** Senior Research Engineer, CRIEPI.

This study is aimed at providing prototype-scale data for two-dimensional beach changes by means of a newly constructed large wave flume. The general similarities and differences between previous and the present experimental results will be discussed. It is shown that net sand transport rate distributions as determined from successive profile changes can be classified into five types, and that these distributions can be simulated by a simple model.

LARGE WAVE FLUME (CRIEPI FLUME)

Flume

The wave flume is shown in Fig. 1. It is made of reinforced concrete, and is 205 m long, 3.4 m wide, and 6 m deep in the 115 m-long generator-side flat section, which is joined to a shoreward section of 1/15 slope. The top of the flume is 1.5 m above ground level. Trucks for carrying or dumping bed materials can be driven in directly through the access slope adjacent to the end of the flume. The wave generator is of the piston type as shown in Fig. 2, with no water behind the blade. Seals for preventing water infiltration are installed along the side and bottom edges of the blade. The blade is driven by oil pressure supplied from two pumps, each driven by a 370 kw electric motor under the control of an electric-hydraulic servo mechanism. The system is capable of producing waves up to 2 m in height.

Because the blade and its supporting frame are fairly heavy (weighing a little over 10 ton), unusually rapid motion is dangerous. Therefore, an automatic, slow starter-stopper was installed. In the event that either an earthquake, water leakage, oil pressure drop, excess oil temperature rise or an overload is sensed, the blade automatically stops and the cause is indicated by lamps on the control board in the operation room. Usually the flume is run from the operation room near the center and at the side of the flume. In addition, the flume is equipped with a vehicle for measurement, and filtration equipment (maximum capacity: 120 m^3/hr).

Wave Generator

An example of waves generated in the flume is given in Fig. 3. The wave generator is designed to produce a maximum wave 2 m in height and 5 s in period in a water depth of 4.5 m, according to the wave generation theory of Biesel and Suquet (1951). Because a very large thrusting force is required, the hydrostatic force is compensated by two balancing actuators (each with maximum thrust force of 40 ton), and the dynamic force to produce waves is generated by a servo-actuator (maximum thrust force is 30 ton). The stroke length needed for the maximum wave is 2200 mm. The compensation of the volume change in the balancing cylinders and the oil pressure variation in the servo-valve is done by the accumulators. The maximum stroke length of the actuators is as 2400 mm including a $\pm$100 mm allowance. The displacement of the piston of the servo-actuator is detected through a rack and pinion gear, and counted by a rotary encoder.

For the surface contact of the water seals, a high-polymer tape 24 mm in width and possessing a very low friction coefficient is used. The tape is kept in contact with the slipping wall of the flume by air

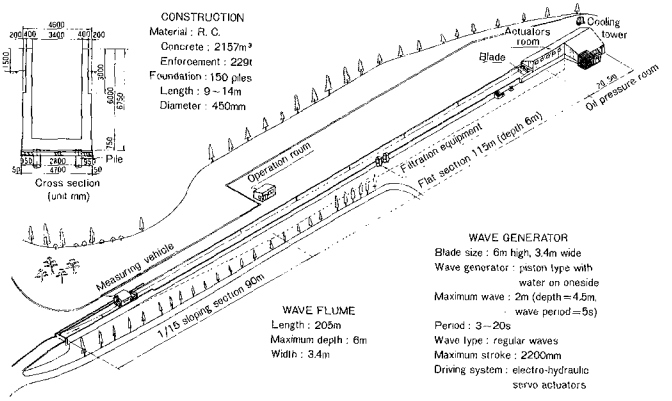

Fig. 1 Prototype wave flume for beach change experiment.

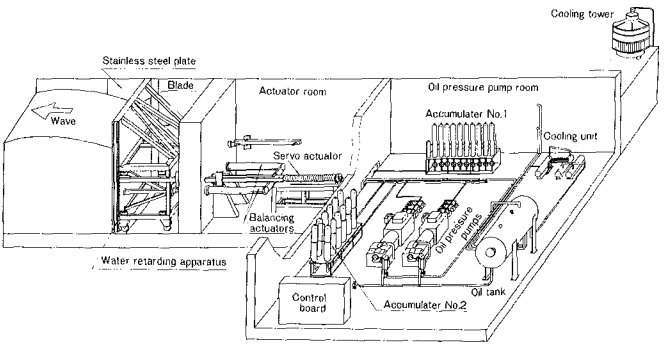

Fig. 2 Wave generator.

Fig. 3 Waves in the flume.

Table 1 Comparison of various types of wave gauges.

Wave gauge	Before breaking			After breaking		
	Error* (%)	Response	Operation	Error* (%)	Response	Operation
Ultrasonic type (under water)	4.2	A	D			D
Ultrasonic type (in the air)	−2.4	A	A	−5.9	C	A
Resistance type	−2.8	A	A	−8.0	D	C
Capacitance type-1	−7.0	B	A	−1.6	C	C
Capacitance type-2	4.5	A	A	−0.6	A	C
Buoy type	8.2	D	B			D
Pressure type (strain gauge)	6.8	D	B	−3.8	D	D

* : Relative error in wave height
A : Good
B : Acceptable
C : Marginally accaptable
D : Unacceptable

pressure (1.5 kg/cm^2) transmitted through waterproof urethane rubber. For reducing wear of the tape, the surface of the slipping wall of the flume is faced with stainless steel plates 5 mm thick.

Measuring System

The wave flume is equipped with a measuring vehicle (weight: 5 ton, maximum speed: 45 cm/s). Because measuring devices applicable to the field must be used, a thorough investigation of the accuracy and serviceability of the instrumentation was required. Seven types of wave gauges were tested to determine their suitability. The wave records from the various gauges were compared to the output of a video tape recorder. Characteristics of the gauges are shown in Table 1 (Shimizu et al., 1983). It was decided to use capacitance (type-2) wave gauges and an ultrasonic (in the air-type) wave gauge. For the measurement of water particle velocities, electromagnetic current meters were adopted. Ultrasonic depthmeters with secondary transmitter-receivers for calibration (calibration distance = 200 mm) were used for the subsurface bottom, and a sand surface detector of the surface contact type was also used for the profile above the water level.

The horizontal position of the vehicle and the vertical position of the post supporting the depthmeter are detected using rotary encoders. The depth was measured every 50 mm in the horizontal direction by raising or lowering a post according to the output of the depthmeter while moving the vehicle. For the measurement of the microscale topography such as sand ripples, the same system was utilized except that the sampling interval was reduced to 1 mm. The data acquisition system on the carrier is controlled by a 20 kB microcomputer. For data processing, mainframe computors (FACOM M200 and M160F) are used.

EXPERIMENTAL RESULTS

Procedure

Coarse sand (median diameter D_{50} = 0.47 mm) and fine sand (D_{50} = 0.27 mm) were used in the experiments. Material properties are summarized in Table 2. Initial profiles of all cases were formed as uniform slopes of $\tan\beta$ (= 5/100 or 3/100). Conditions of the test cases are summarized in Table 3. The water depth at the flat section of the flume was 3.5 m in CASES 2-1 to 2-3, while in the other cases this depth was 4.5m.

Measurements were made of the beach profile, wave height, water velocity and time-averaged concentration of suspended load. The breaking point, breaker type, run-up point, run-down point and number of waves in the surf zone were also observed. In general, measurements of the beach profile were made along the center line of the wave flume. In order to examine the two-dimensionality of the beach profiles, measurements of the beach profile in CASE 1-1 were made along three lines; one was the center line of the flume, and the others were 1.1 m to either side of the center line. It was found that the difference between measured profiles was within $\pm$5 cm. It was thereby confirmed that the measurement profile along the center line represents the two-dimensional beach profile in the wave flume.

Table 2 Properties of sand.

Material			coarse sand		fine sand	
Median diameter D_{50} (mm)			0.47		0.27	
Sorting coefficient $So=\sqrt{D_{75}/D_{25}}$			1.57		1.35	
Skewness parameter $Sk=\sqrt{D_{25}D_{75}}/D_{50}$			1.03		1.03	
Specific gravity			2.69		2.71	
Void ratio	wet sand	compacted	34 %	39 %	35 %	41 %
		not compacted	43 %		46 %	
	dry sand	compacted	34 %	37 %	39 %	41 %
		not compacted	39 %		43 %	
Angle of repose		underwater	33°		33°	
		in the air	33°		32°	

Table 3 Conditions and test cases.

CASE	Median diameter of sand D_{50} (mm)	Initial slope tan β	Wave period T (s)	Wave height* Ho (m)	Duration of wave action t (hr)
1-1	0.47	5/100	6.0	0.46	20.0
1-3			9.0	0.95	69.5
1-8			3.0	0.85	21.0
2-1		3/100	6.0	1.76	35.0
2-2			9.0	0.73	39.0
2-3			3.1	0.71	29.4
3-1	0.27	5/100	9.1	1.07	71.0
3-2			6.0	1.05	98.1
3-3			12.0	0.65	80.0
3-4			3.1	1.62	76.1

* Ho is estimated from the wave height at the uniform depth section.

Beach Profile Change

Figure 4 shows beach profiles at the final stages. Saville (1957) also conducted experiments using a prototype-scale wave flume, and published profiles of four cases. The profile of his case, T = 11.33 s, H = 1.8 ft, closely resembles the present CASE 3-1. In the other three cases, the beach profile changes reached the toe of the slope. In Fig. 4, it can be seen that profiles in most of our cases were not affected by the finite length of the slope. In laboratory experiments (e.g., Sunamura and Horikawa, 1974), accretion outside the surf zone is often observed under conditions of fine sand and steep slope. But in our cases corresponding to this situation (CASE 3-1 to CASE 3-3), erosion occurred outside the surf zone. In CASE 3-4, accretion occurred outside the surf zone, but the beach profile was considerably different from typical laboratory experimental results, especially near the bar.

In Fig. 4, locations of breaking points are indicated by triangles, an open triangle for the initial stage, and a solid triangle for the final stage. Plunging breakers were observed in almost all cases, except that plunging breakers with some characteristics of collapsing or spilling breakers were observed in CASE 1-3 and CASE 3-4, respectively. Battjes (1974) classified breaker types using the surf similarity parameter ξ_o,

$$\xi_o = \tan\beta \,/\sqrt{H_o/L_o} \tag{1}$$

where $\tan\beta$ is the beach slope, and H_o and L_o are the wave height and wave length in deep water, respectively. The critical value between spilling and plunging breakers was given as $\xi_o = 0.5$. However, in the present experiments, at the initial state of beach profile change the critical value was found to be $\xi_o = 0.15$. (A detailed discussion is given by Maruyama et al., 1983)

In CASES 2-1, 2-2, and 2-3, all with a gentle slope of $\tan\beta = 3/100$, secondary breaking was observed, particularly in CASE 2-1 shown in Fig. 5. Bars were formed in all cases and, in CASE 2-1 a smaller bar also formed near the secondary breaking point. In addition, a berm formed in all cases except for CASE 1-8 and CASE 3-4.

Sunamura and Horikawa (1974) found that shoreline changes could be classified by means of the nondimensional parameter C:

$$C = (H_o/L_o)\,(\tan\beta)^{0.27}\,(D_{50}/L_o)^{-0.67} \tag{2}$$

where, $\tan\beta$ is the average beach slope from the initial shoreline up to the critical water depth of sediment movement. In the present paper, $\tan\beta$ is equivalent to the uniform slope of the initial beach. The demarcation value of C between recession and advance of shoreline was 4 - 8 for laboratory measurements, and 9 - 18 for field measurements. Sunamura (1980a) eliminated noncredible data and added new data, and found that the demarcation value of C for field data was 18.

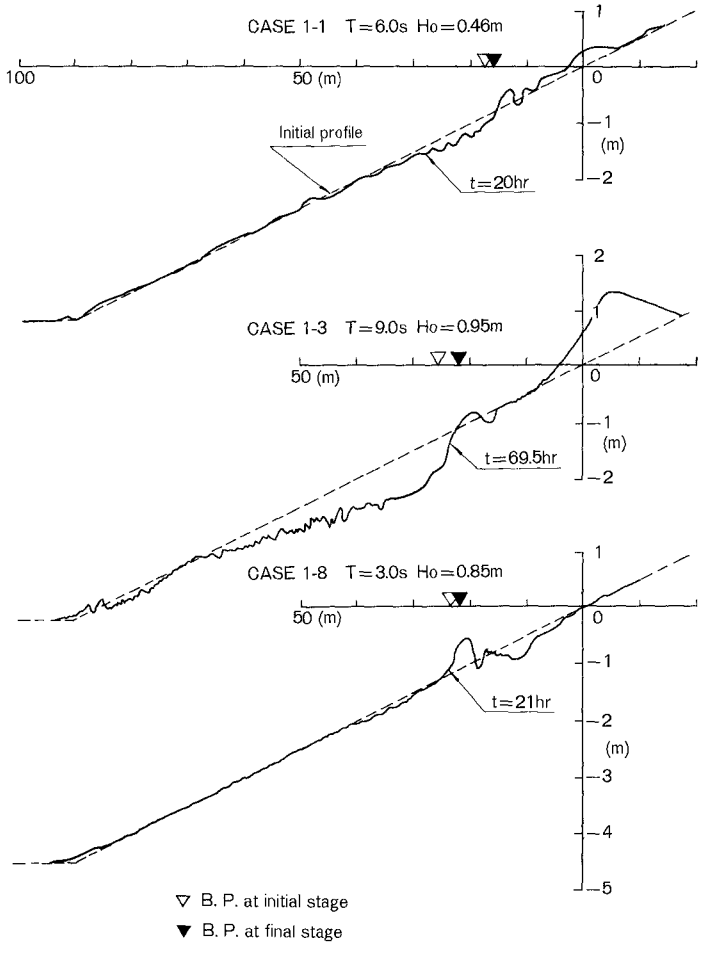

Fig. 4(a) Beach profile changes (steep beach with coarse sand).

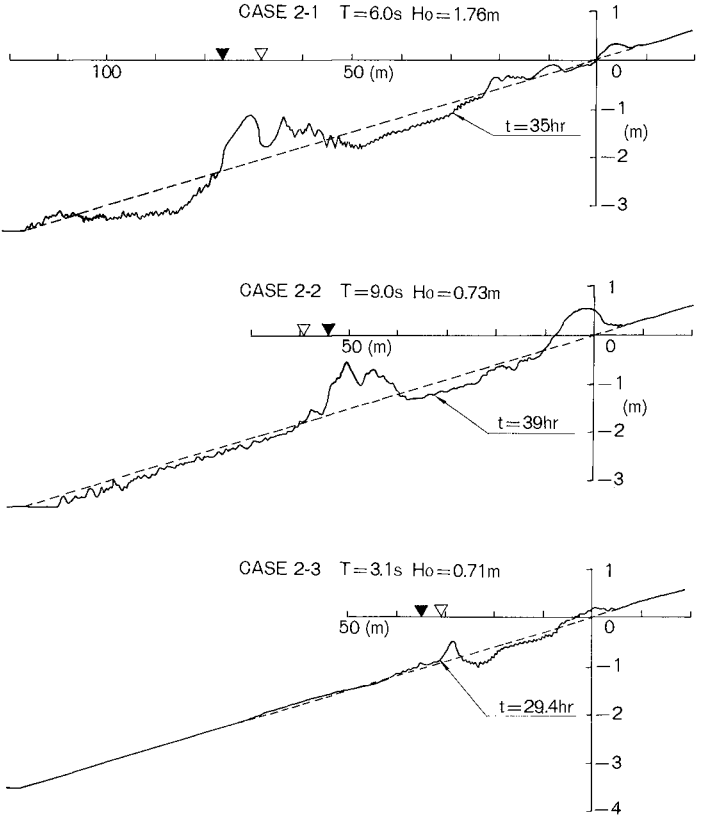

Fig. 4(b) Beach profile changes (gentle beach with coarse sand).

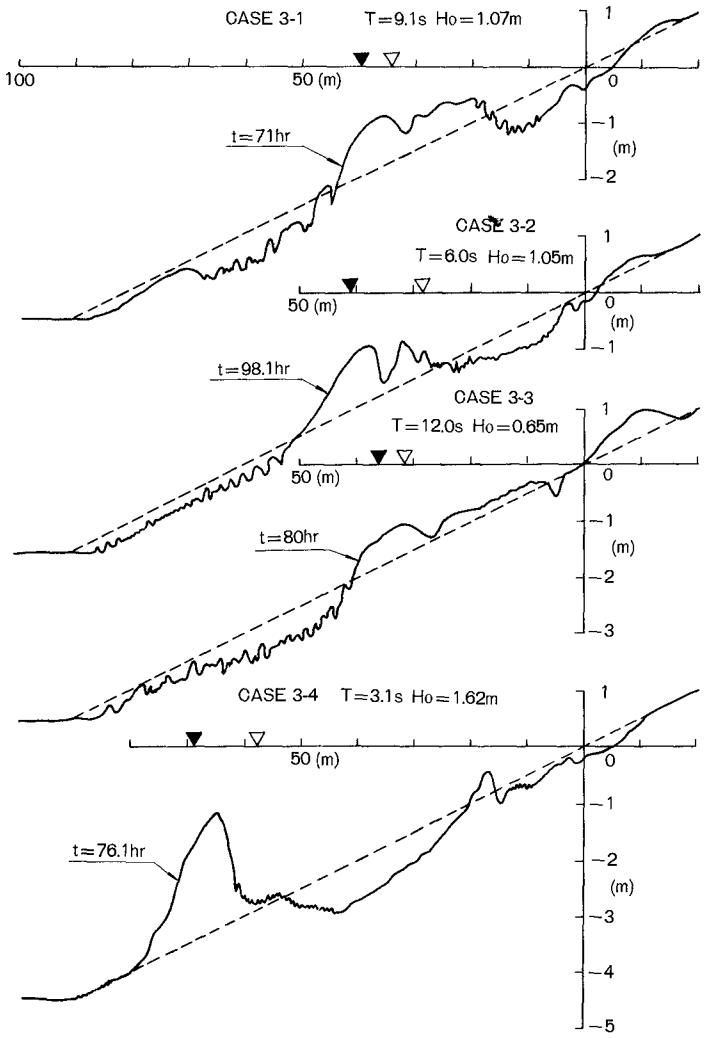

Fig. 4(c) Beach profile changes (steep beach with fine sand).

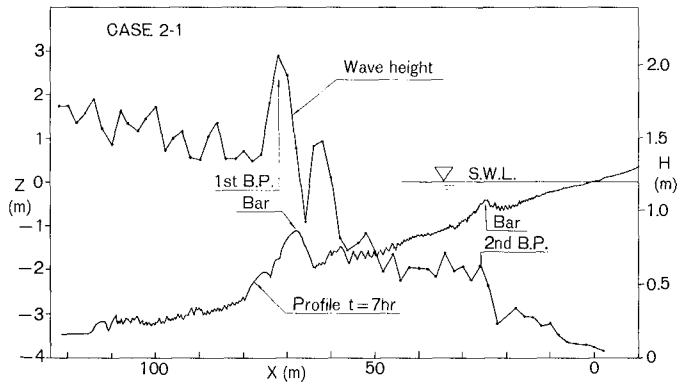

Fig. 5 Distribution of wave height in CASE 2-1.

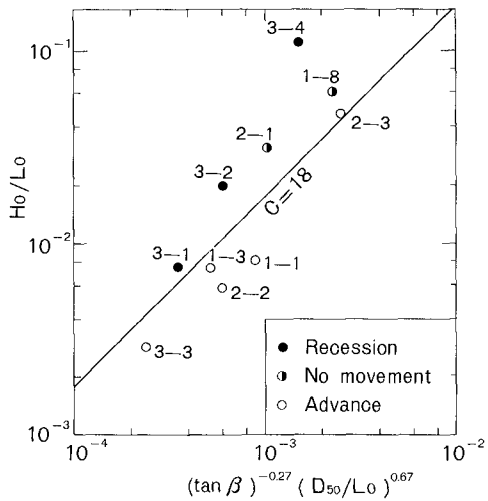

Fig. 6 Classification of shoreline change.

The results of applying this method to the present data are shown in Fig. 6. The transition from recession to advance of the shoreline is defined by C = 18, which is similar to the field data result. Consequently, the authors consider that processes of beach profile change in this wave flume are similar to those in the prototype. In CASES 1-8 and 2-1, by consideration of the parameter C, the shoreline was expected to recede. However, this situation did not occur (as shown in Fig. 6). It is believed that the shoreline change was produced by the waves near the shoreline rather than the deep water waves. In CASE 2-1, secondary breaking might also have influenced the shoreline change.

The critical water depths at which noticeable profile changes were observed are compared with the results of some previous studies described by Horikawa (1978) in Fig. 7. The results for CASE 2-2, CASE 3-2 and CASE 3-4 are excluded because in CASE 2-2 and CASE 3-2 the profile changes extended to the toe of the slope, and in CASE 3-4 the profile change did not reach the equilibrium state. It was found that the critical water depths for profile change agreed with the criterion of completely active movement given by Sato and Tanaka (1962), namely,

$$H_o/L_o = 1.35\,(D_{50}/L_o)^{1/3}\,(\sinh 2\pi h/L)\,(H_o/H) \tag{3}$$

where, h is the critical water depth of sediment movement and H and L are the wave height and wave length at the water depth h, respectively.

Net Sand Transport Rate

Net sand transport rate distributions for each case were calculated from successive beach profiles. Beach profiles and distributions were classified into three types as shown in Fig. 8. Type I (erosion type), Type II and Type III (accretion type) correspond to the beach profile classification of Sunamura and Horikawa (1974). In addition, the present experimental results for Type I and Type III were subdivided into Mono-crested and Bi-crested types. Bi-crested distributions of Type I and III tend to transform to Mono-crested distributions with time as the breaking point moves seaward or shoreward.

It was found that each type of net sand transport rate distribution could be classified according to the parameter C, as plotted in Fig. 9. The condition of transition from Type I to Type III occurs at C = 18. Furthermore, the Mono-crested and Bi-crested distributions could be classified by a newly proposed parameter P as follows:

$$\left.\begin{array}{ll} \text{Mono-crested distribution} & P > 10^{-3} \\ \text{Bi-crested distribution} & P < 10^{-3} \end{array}\right\} \tag{4}$$

$$P = (\tan\beta)^{-0.27}\,(D_{50}/L_o)^{0.67} \tag{5}$$

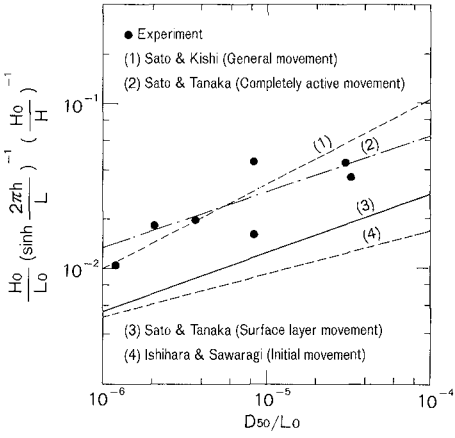

Fig. 7 Comparison between experimental results and various expression for sediment movement inception.

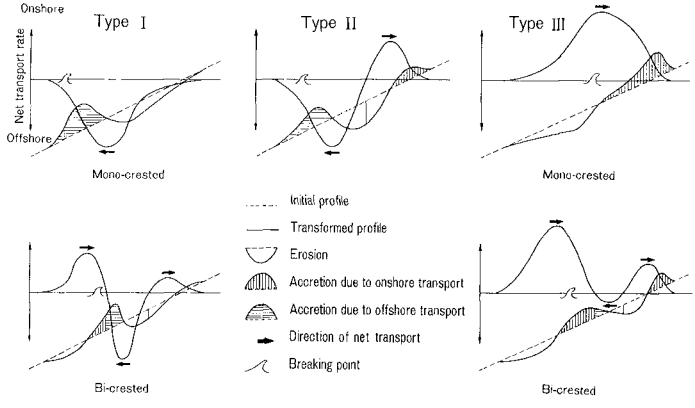

Fig. 8 Types of net transport rate distributions.

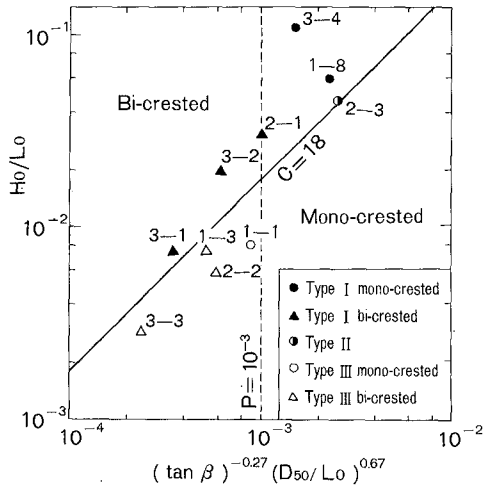

Fig. 9 Net transport rate distribution types classified by parameter C and P.

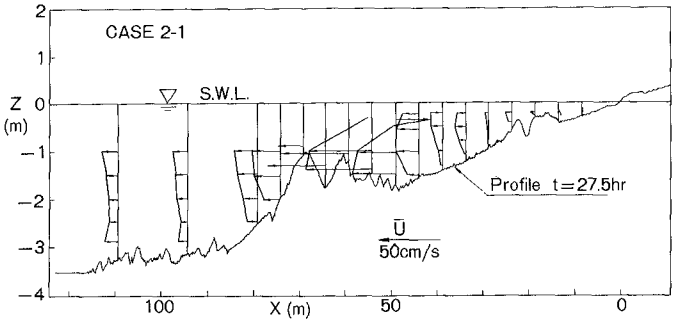

Fig. 10 Distribution of time averaged horizontal velocity of CASE 2-1.

Sawaragi and Deguchi (1980) classified into four types the net transport rate distributions obtained in rather small-scale experiments. Type II-2 of their classification corresponds to the Bi-crested distribution of our prototype-scale experiments. However, in laboratory experiments, Bi-crested types are rarely observed. One reason for this discrepancy may be that values of the parameter P in such laboratory experiments are different from those in prototype-scale experiments. For example, in almost all laboratory experiments conducted by Sunamura and Horikawa (1974), P was greater than 10^{-3}.

MODEL OF BEACH PROFILE CHANGE

At the present time, motions of the waves and fluid near and inside the surf zone have not been examined in sufficient detail to estimate the net sand transport rate directly from these quantities. Accordingly, as a first step in grasping the overall magnitude of sand transport in the present experiments, we constructed a rather simple model that directly relates the distribution of the net transport rate with the conditions of the waves and the beach, using the data corresponding to the cases with coarse sand (D_{50} = 0.47 mm). [Swart (1974) and Sunamura (1980b) proposed models based on the same basic ideas. However, application of their models is restricted only to erosional beaches, and consequently, their models can not express the growth of bars and berms.]

In the present model, it is assumed that the distribution of on-offshore sand transport rate Q (transport rate per unit width perpendicular to wave propagation) extending from the swash zone to outside the surf zone can be interpreted as the sum of relatively independent components of net sand transport (Q_1, Q_2 and Q_3) as follows,

$$Q = Q_1 - Q_2 + Q_3 \tag{6}$$

where

Q_1: net onshore transport outside the surf zone caused by nonlinearity of the fluid motion under waves

Q_2: net offshore transport inside the surf zone caused by time-averaged seaward-directed currents

Q_3: net onshore transport in the swash zone caused by wave run-up.

Figure 10 shows a typical distribution of time-averaged horizontal velocity for CASE 2-1. Strong seaward currents were observed throughout the surf zone, and the maximum velocity of these currents reached about 0.5 m/s. It is believed that these seaward currents have a great influence on the net sand transport rate Q_2.

The five types of net transport rate distributions shown in Fig. 8 then correspond to different relative magnitudes of the above components. According to the assumptions, the net transport rate distribution can be expressed as follows:

$$Q = Q_1 - Q_2 + Q_3$$

$$= A_1 \exp[-((x-x_1)/B_1x_b)^2] - A_2 \exp[-((x-x_2)/B_2x_b)^2] + A_3 \exp[-((x-x_3)/B_3x_b)^2] \quad (7)$$

Here x is the distance from the shoreline of the initial beach profile, and x_b denotes the breaking point. In Eq. (7), 1st term gives a peak A_1 near the breaking point ($x = x_1$); the 2nd term gives a peak A_2 near the center of the surf zone ($x = x_2$); and the 3rd term gives a peak A_3 near the shoreline ($x = x_3$). Each Gaussian distribution has a characteristic width of B_1, B_2, and B_3, respectively. For example, if either B_1, B_2 or B_3 is equal to 0.2, the width of the distribution is nearly equal to the width of the surf zone.

It is also assumed that the peaks A_1, A_2, and A_3 decrease exponentially with time from their initial values of A_{10}, A_{20} and A_{30},

$$A_1 = A_{10} \exp[-\alpha_1 t], \quad A_2 = A_{20} \exp[-\alpha_2 t], \quad A_3 = A_{30} \exp[-\alpha_3 t] \quad (8)$$

where t is the time, and α_1, α_2 and α_3 are decay coefficients. The tendency of the net transport rate distribution to transform from Bi-crested to Mono-crested types may be simulated by means of α_1, α_2 and α_3.

The continuity equation of two-dimensional beach profile change is

$$\frac{\partial h}{\partial t} = -\frac{\partial Q}{\partial x} \quad (9)$$

where h is water depth. Therefore, substituting Eq. (7) into Eq. (9) and integrating Eq. (9) over time starting from the initial beach profile, the beach profile at a given time can be obtained.

The initial distributions of net transport rate corresponding to the cases with coase sand were calculated from the difference between the initial profiles and those after three hours, and A_{10}, A_{20}, and A_{30} were determind by the least squares method. The results are shown in Table 4. In determination of these values, B_1, B_2 and B_B were assumed as shown in Table 4.

Table 4 Parameters of the model.

CASE	1—1	1—3	1—8	2—1	2—2
χ_b (m)	18.0	26.2	22.8	69.2	57.5
χ_1 (m)	24.8	32.7	27.8	78.4	57.5
χ_2 (m)	18.8	14.7	19.8	64.4	37.5
χ_3 (m)	0.8	−1.3	5.8	29.4	5.5
B_1	0.45	0.45	0.15	0.15	0.45
B_2	0.30	0.30	0.075	0.075	0.30
B_3	0.15	0.15	0.30	0.30	0.15
A_{10} (m^3/hr/m)	0.83	1.28	0.14	1.91	0.68
A_{20} (m^3/hr/m)	0.49	−0.26	1.11	2.65	0.22
A_{30} (m^3/hr/m)	0.11	1.18	−0.06	0.33	0.45

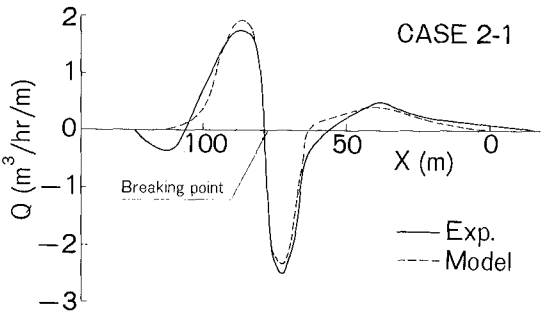

Fig. 11 Net transport rate distribution approximated by Eq. (7).

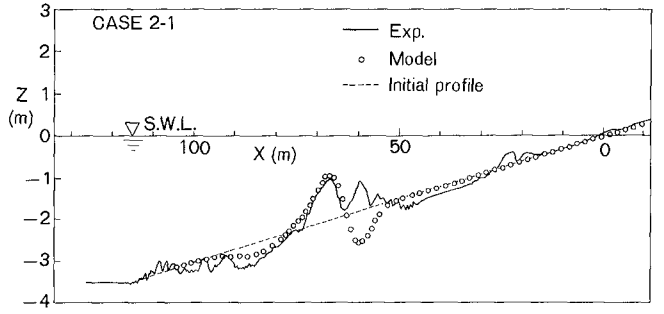

Fig. 12 Beach profile calculated by the model.

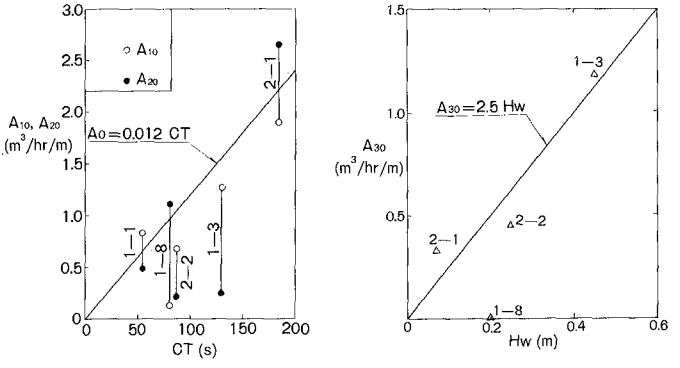

Fig. 13 Properties of the initial peak parameters A_{10} to A_{30}.

An example of the net transport rate distribution approximated by Eq. (7) is compared with the measured distribution in Fig. 11. It was found that the distributions of net transport rate in the other cases were also well approximated by Eq. (7).

Figure 12 is an example of the predicted from Eq. (9) and measured profiles for CASE 2-1 after 20 hours of wave action. The profile change outside the surf zone is well simulated by this model. On the other hand, the local profile change near the plunging point is not so well reproduced. In numerical calculation, the assumption was employed that the locations x_i, where each transport rate component Q_i has a peak, do not move when the bottom profile changes. To improve this model, therefore, it is necessary to take account the effect that the center of the Gaussian distribution of each component of Q can move with changes in the beach profile.

In order to generalize the present model, the dependence of the parameters A_{10}, A_{20} and A_{30} on the experimental conditions was investigated. The results are shown in Fig. 13. The parameter A_{10} in the accretionary cases and A_{20} in the erosional cases, which correspond to the most dominant components, appear to have a positive correlation with the product of the parameter C and the wave period T. The parameter A_{30}, which represents the onshore transport in the swash zone, appears to be related to the wave height at the shore-line H_w.

CONCLUSIONS

1) Shoreline change in these prototype-scale experiments was predicted by the parameter C (Eq. 2) of Sunamura and Horikawa (1974). The demarcation value of C separating recession and advance was confirmed to be 18 (Fig. 6).

2) The critical water depth of the beach profile change agreed well with the criterion of completely active movement (Eq. 3) given by Sato and Tanaka (1962).

3) The observed net transport rate distributions were classified into 5 types (Fig. 8). They could be identified by the parameters C and P (Fig. 9).

4) The net transport rate distributions were well approximated by the sum of three Gaussian distributions (Eq. 7). The parameters of this model were related to the wave and beach conditions (Fig. 13).

ACKNOWLEDGMENTS

We would like to extend our appreciation to Professor K. Horikawa, University of Tokyo, and Professor S. Hattori, Chuo University, for valuable discussions and advice. We are also grateful to Professor Nath, Oregon State University, for kindly supplying information about the wave flume at that institution. In addition, we would like to thank Dr. N. C. Kraus, Nearshore Environment Research Center, for critically reading the manuscript, and Miss T. Kohno for typing.

REFERENCES

1) Battjes, J.A.: Surf similarity, Proc. 14th Coastal Eng. Conf., ASCE, pp. 466-480, 1974.

2) Biesel, F. and F. Suquet: Les appareils générateurs de houle en laboratoire, La Houille Blanche, No. 2, pp. 147-165, 1951.

3) Horikawa, K.: Coastal Engineering, University of Tokyo Press, and Halsted Press, 402pp., 1978.

4) Maruyama, K., T. Sakakiyama, R. Kajima, S. Saito and T. Shimizu: Experimental study on wave height and water particle velocity near the surf zone using a large wave flume, Civil Eng. Lab. Rep. No. 382034, CRIEPI, 1983. (in Japanese)

5) Sato, S. and T. Tanaka, 1962. (see Ref. 3)

6) Saville, T. Jr.: Scale effects in two dimensional beach studies, Proc. 7th General Meeting, IAHR, pp. A3.1 - 8, 1957.

7) Sawaragi, T. and I. Deguchi: On-offshore sediment transport rate in the surf zone, Proc. 17th Coastal Eng. Conf., ASCE, pp. 1194-1214, 1980.

8) Shimizu, T., K. Maruyama, R. Kajima and S. Saito: Characteristics of field type measuring equipments tested in a large wave flume — wave gages, current meters, and depthmeters —, Civil Eng. Lab. Rep., CRIEPI, 1983. (in preparation, in Japanese)

9) Sunamura, T.: Predictive model for shoreline-position change on natural beaches, Proc. 27th Japanese Conf. on Coastal Eng., JSCE, pp. 255-259, 1980a. (in Japanese)

10) Sunamura, T.: A laboratory study of offshore transport of sediment and a model for eroding beaches, Proc. 17th Coastal Eng. Conf., ASCE, pp. 1051-1070, 1980b.

11) Sunamura, T. and K. Horikawa: Two dimensional shore transformation due to waves, Proc. 14th Coastal Eng. Conf., ASCE, pp. 920-038, 1974.

12) Swart, D.H.: A schematization of onshore-offshore transport, Proc. 14th Coastal Eng. Conf., ASCE, pp. 884-900, 1974.